

## LONG-TERM EARTHQUAKE FORECAST FOR IRAN

Mohammad TALEBI

*Ph.D. Student, International Institute of Earthquake Engineering and Seismology (IIEES), Tehran, Iran.  
m.talebi@iiees.ac.ir*

Mehdi ZARE

*Associate Professor, International Institute of Earthquake Engineering and Seismology (IIEES), Tehran, Iran.  
mzare@iiees.ac.ir*

Anooshiravan ANSARI

*Assistant Professor, International Institute of Earthquake Engineering and Seismology (IIEES), Tehran, Iran.  
a.ansari@iiees.ac.ir*

**Keywords:** Probabilistic Earthquake Forecasting, Adaptive Kernel, Iran

### ABSTRACT

We present a model of earthquake forecasting in Iran to assess the long-term probabilities of future earthquakes with moderate and large magnitudes ( $M \geq 5.5$ ). The model estimates a coupled rate of magnitude, space and time for future seismicity using a spatial-temporal Poisson process. We applied the ISC bulletin for the selected region (latitude  $25-41^\circ$  and longitude  $43.5-64^\circ$ ) in the period of 1970 to 2012. Our results show a meaningful correlation between anomalies of the forecasted seismicity map and the epicenters of target events occurred from 2013 to 2014. Based on the results, we have concluded that the anomalies of the forecasted map should be considered as high risk regions.

### INTRODUCTION

Iranian plateau is one of the most seismically active regions in the world and it frequently suffers catastrophic earthquakes. They cause heavy loss of human life along with lots of property damages because of the poor quality of constructions in Iran.

In this study, we have investigated the occurred earthquakes in this region from 1970 to 2012 in order to estimate the probability of future moderate and large magnitude events ( $M \geq 5.5$ ) in a five-year period (forecasted seismicity map). The earthquakes occurred in the period of 2013-2015 has also been applied for validity test of the forecasted seismicity map.

### DATA

We applied the regional data sets of the International Seismological Centre (ISC). This catalog is available at <http://www.isc.ac.uk/>. The ISC's reviewed earthquake origins are typically available about two

years in arrears and are intended to be as comprehensive as possible. The ISC provides a large number of magnitude types that can be divided into 3 main groups: 1) teleseismic, 2) complementary magnitude, and 3) local magnitude. Within the Iranian territory, the magnitude  $M_s$  (surface wave magnitude) is reported for most of the events (53%), whereas  $M_L$  is provided for about one-third of them (32%). We used the ISC catalog in the period of 1970 to 2014. Here, we simply considered the local magnitude ( $M_L$ ) and body wave magnitude ( $M_b$ ) of  $M < 6$  as well as surface wave magnitude ( $M_s$ ) of  $M > 6$  as moment magnitude.

We selected earthquakes within a rectangular, latitude limits  $25^\circ$ -  $41^\circ$  and longitude limits  $43.5^\circ$ -  $64^\circ$ . The magnitude of completeness ( $M_c$ ) was checked by the maximum curvature function based on the study of Wiemer and Wyss (2000). The  $M_c$  selected is 4.5 at the 95% confidence level (figure 1).

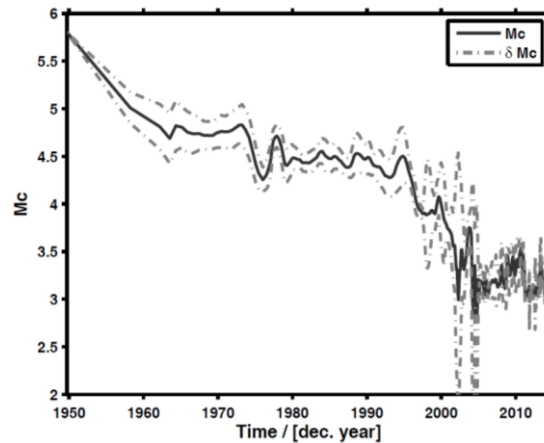


Figure 1. Temporal variation of  $M_c$  using maximum curvature function.

## DECLUSTERING

In order to remove large obscures of seismic activity, earthquake catalogue can be declustered. The applied catalog was declustered by the Reasenberg's algorithm (1985) as modified by Helmstetter et al. (2007). We only changed error values of epicenter and depth location to 5 and 7 km, respectively. Other parameters are considered as given in Helmstetter et al. (2007). The declustering procedure found 770 clusters of earthquakes; a total of 5178 events (out of 19224). The resulting declustered catalog has 14816 events. Spatial distributions of earthquakes listed in the declustered catalog are shown in figure (2).

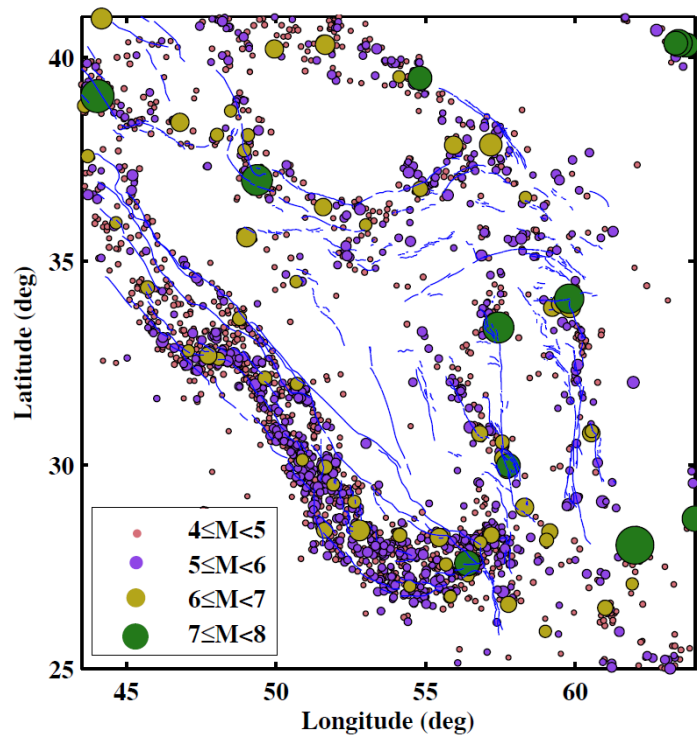


Figure 2. Epicenter locations of earthquakes with  $M \geq 4.5$  listed in the declustered catalog in the period of 1970 to 2014. Major tectonic features are also shown by solid lines.

Figure (3a) also shows temporal distributions of earthquake in the raw and declustered catalogs, respectively. The cumulative number curve as a function of time for the refined catalog with  $M \geq 4.5$  has a smoother slope compared with the raw catalog and illustrates that the declustering procedure has removed most of the dependent events from the catalog. It is obvious that the resulting declustered catalog is still a little clustered in space and time, as the parameters of the declustering algorithm were used to eliminate large fluctuations of seismicity. However, the remained clusters commonly happen at a small spatial-temporal scale. Hence, the estimations from this declustered catalog over large scales can be a good evaluation of the long-term properties of seismicity.

The Gutenberg-Richter relation was found to be  $\log N = 7.59 - 0.93 * M$  (figure 3b). The b-value and a-value have been estimated as 0.93 and 7.59, respectively. The tectonic earthquakes are characterized by the b-value from 0.5 to 1.5 and are more frequently around 1.0 (Mogi, 1967). So, our observation almost agrees with typical size scaling b and a-values.

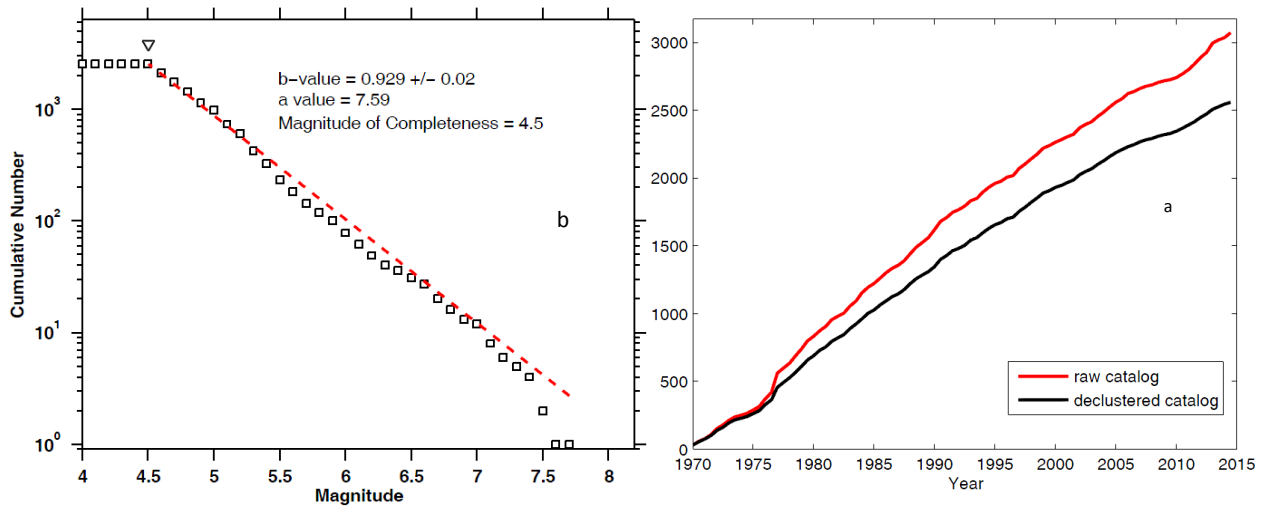


Figure 3. a) Temporal distributions of earthquake in the raw and declustered catalogs. b) Frequency magnitude distribution of events for the declustered catalog.

## METHOD

### a. SMOOTHENED SPATIAL DISTRIBUTION OF SEISMICITY

Spatial density of seismicity was estimated by smoothing the locations of earthquakes with  $M \geq 4.5$ . We used an isotropic adaptive kernel for smoothing past earthquake locations. As it is used in several studies (e.g. Helmstetter et al., 2007; Werner et al., 2011), a power-law type kernel was used as follows:

$$K_d(r) = \frac{C(d)}{(|r|^2 + d^2)^{1.5}} \quad (1)$$

Where  $r$  is epicentral distance of  $i$ -th event for each grid point,  $d$  is the adaptive scale parameter, and  $C(d)$  is normalization constant set so that the integral of the kernel over an infinite area equals 1.0. In figure (4), we illustrate the use of the kernel to evaluate the smoothed rate of earthquakes.

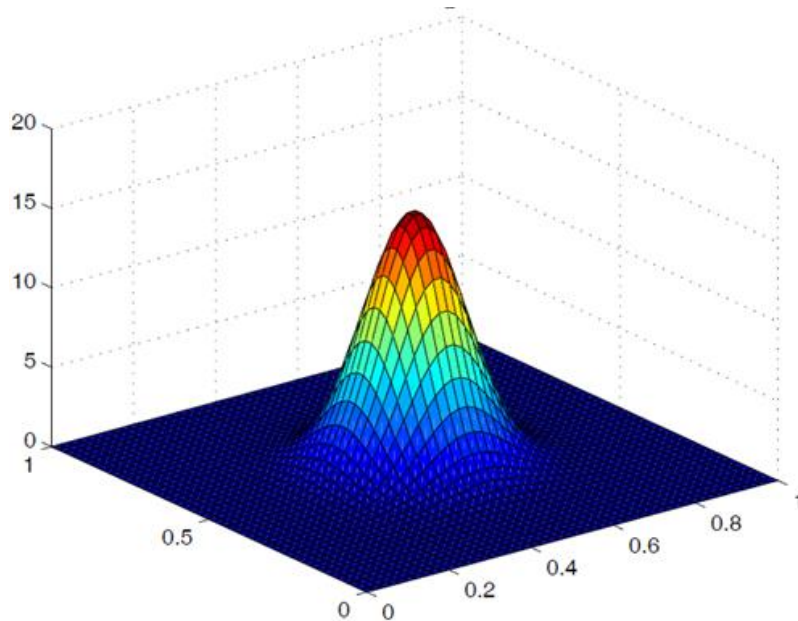


Figure 4. Schematic diagram of an isotropic power-law kernel

The density ( $\lambda$ ) at each point was estimated by summing the portion of all past earthquakes ( $N$ ) as follows:

$$\lambda = \sum_{i=1}^N K_d(r) \quad (2)$$

The bandwidth ( $d$ ) of the kernel was adjusted regarding the horizontal distance of  $n$ -th nearest neighbor of each earthquake. The number  $n$  was an adaptable parameter that was evaluated by optimizing the model. The bandwidth decreased if the spatial seismic distribution was large in size around the location of  $i$ -th earthquake, so that we had a better resolution where the density increased.

## b. MODEL OPTIMIZATION

We optimized the model by computing the likelihood of the model. Accordingly, we used a Jackknife-like procedure (Kagan and Jackson, 1994) in which the catalog was divided into 2 sub-catalogs. We applied the first sub-catalog, as learning catalog, to forecast the second sub-catalog, as test catalog.

## c. EXPECTED NUMBER OF EVENTS IN MAGNITUDE BINS

The spatial density was scaled to the number of expected earthquakes by using expected number of earthquakes over a year. Then, to estimate a magnitude-dependent rate, we multiplied the scaled spatial density by a tapered Gutenberg-Richter magnitude frequency distribution. Finally, to obtain the long-term forecast, we scaled the calculated rate by the number of years. Figure (5) shows the forecasted seismicity rate ( $M \geq 5.5$ ) map of Iran for five-year period from January 1, 2013, based on the ISC catalog.

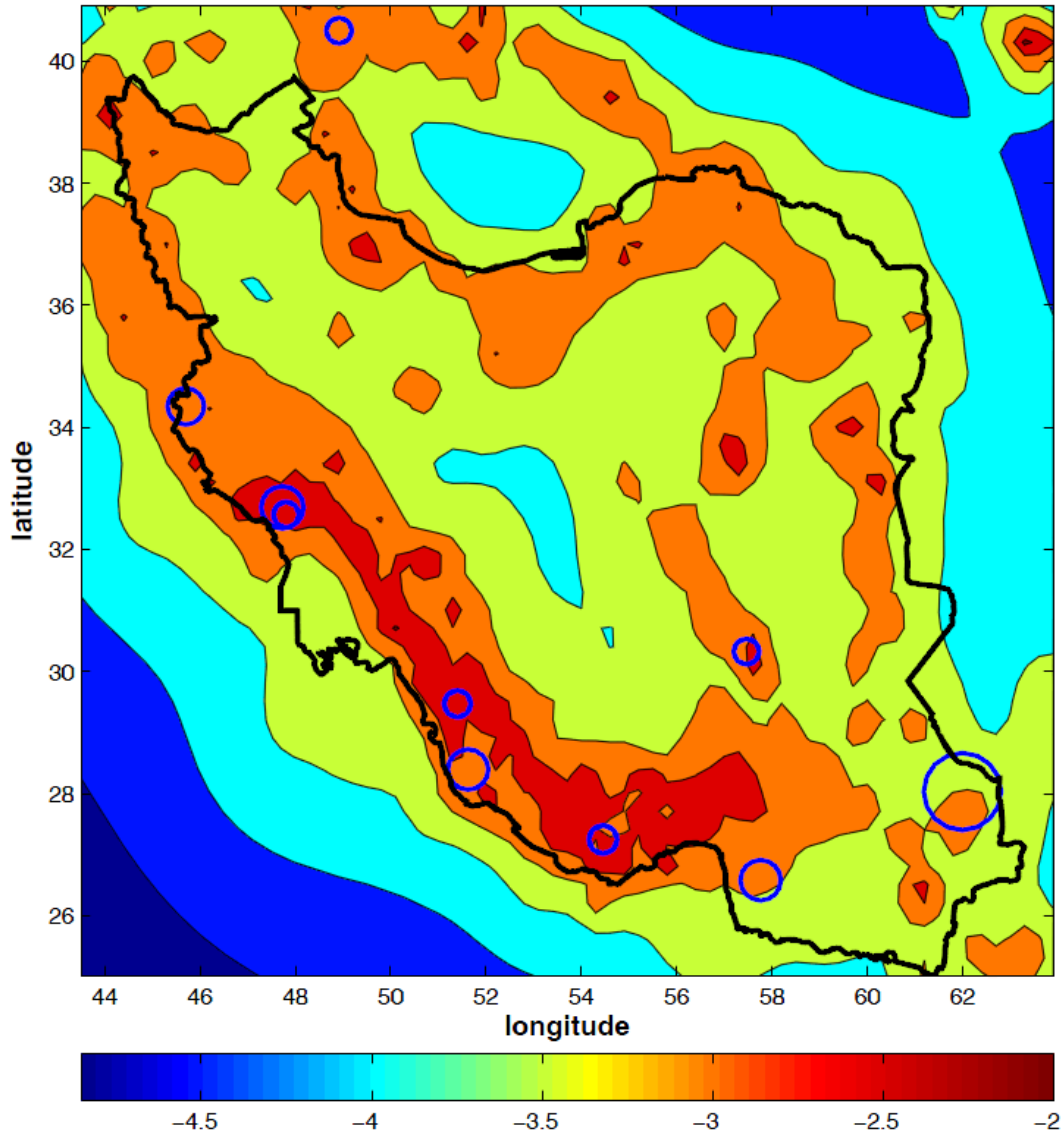


Figure 5. The base 10 logarithm of expected number of earthquakes with  $M \geq 5.5$  over the five-year period from January 1, 2013 based on smoothing the locations of earthquakes of  $M \geq 4.5$  in the ISC catalog from 1970 to 2013. Black line shows Iran border and circles are  $M \geq 5.5$  main earthquakes that occurred between 1 January 2013 and 20 September 2014.

## DISCUSSION AND CONCLUSION

We have defined the most likely candidate spaces for upcoming events with  $M \geq 5.5$  over the five-year period from January 1, 2013. Figure (5) shows the meaningful correlation between forthcoming events and the calculated anomalies of the forecasted seismicity rate map. Hence, we can conclude that the probable forthcoming earthquakes could be occurred in regions with the highest forecasted seismicity rates and special attention should be given to these anomalies.

## REFERENCES

- Helmstetter A, Kagan YY and Jackson DD (2007) High resolution time-independent grid-based forecast for  $M \geq 5$  earthquakes in California. *Seism. Res. Lett.*, 78(1), 78-86
- Kagan YY and Jackson DD (1994) Long-term probabilistic forecasting of earthquakes, *J. Geophys. Res.*, 99, 13,685-13,700
- Mogi K (1967) Earthquakes and fractures. *Tectonophysics* , 5, 35-55
- Reasenberg P (1985) Second-order moment of central California seismicity, 1969-82, *J. Geophys. Res.*, 90, 5479-5495
- Werner MJ, Helmstetter A, Jackson DD & Kagan YY (2011) High resolution long- and short-term earthquake forecasts for California, *Bull. seism. Soc. Am.*, 101(4), 1630–1648, doi:10.1785/0120090340
- Wiemer S and Wyss M (2000) Minimum magnitude of completeness in earthquake catalogs: Examples from Alaska, the western United States, and Japan, *Bull. seism. Soc. Am.*, 90, 859–869